

Quantitative comparison of filtering methods in lattice QCD

Falk Bruckmann,¹ Christof Gattringer,² Ernst-Michael Ilgenfritz,³
Michael Müller-Preussker,³ Andreas Schäfer,¹ and Stefan Solbrig¹

¹*Institut für Theoretische Physik, Universität Regensburg, D-93040 Regensburg, Germany*

²*Institut für Physik, FB Theoretische Physik, Universität Graz, A-8010 Graz, Austria*

³*Humboldt-Universität zu Berlin, Institut für Physik, Newtonstr. 15, D-12489 Berlin, Germany*

We systematically compare filtering methods used to extract topological excitations (like instantons, calorons, monopoles and vortices) from lattice gauge configurations. Each of these techniques introduces ambiguities, which can invalidate the interpretation of the results. We show, however, that all these methods, when handled with care, reveal very similar topological structures. Hence, these common structures are free of artefacts and faithfully represent infrared degrees of freedom in the QCD vacuum. We find an interesting power-law for the clusters of filtered topological charge.

PACS numbers: 11.15.Ha

Introduction

Ever since the advent of quantum chromodynamics (QCD) its infrared properties have been of primary interest. One of the most important phenomena in this regime is the confinement of quarks. As a typical non-perturbative effect it still calls for a derivation from first principles, even for pure gauge theory (where it reveals itself as, e.g., an area law for the Wilson loop).

Remarkably, the most popular nonperturbative approaches to the QCD vacuum have been around for quite some time now. Topological excitations like instantons, calorons, magnetic monopoles and vortices have been used for semiclassical and condensed matter-inspired models since the 70's [1]. In spite of the successes of these models, the question of their relevance for confinement is still controversially debated.

Lattice gauge theory (LGT) is of roughly the same age and till today the only nonperturbative and systematically improvable regulator of QCD. Thus it has the potential to lend support to and to decide between the various models.

However, the QCD vacuum on the lattice as seen by naive gluonic observables has been found to be dominated by ultraviolet (size $O(a)$) fluctuations and therefore it is difficult to make contact to continuum models. To deal with this problem, various smoothing procedures, filtering out the UV 'noise', have been developed and applied to lattice configurations. It has been objected that physical properties could be lost and unphysical artefacts may be generated by these filtering methods. Both effects would strongly spoil the conclusions, for instance w.r.t. the extracted density of the building blocks, drawn from any such study.

In this Letter we systematically investigate the most common and a priori quite different procedures to filter lattice configurations, namely smearing and the modern methods based on the eigenmodes of lattice Dirac and Laplace operators.

We find a surprisingly strong agreement of the topo-

logical content of configurations in thermal equilibrium seen through the different methods. We show how the parameters of the latter can be adapted systematically. This knowledge forms a very important prerequisite to uniquely identify the structure of the QCD vacuum.

Filtering methods

Smearing and the related method of cooling have often been used ad hoc to improve the signal in observables or to obtain smoother link variables as input for lattice operators. For definiteness here we will use APE-smearing, that has been argued to be equivalent to RG cycling [2]. It is an iterative procedure, where links are replaced by a weighted average of the links and the staples $U_\mu^\nu(x) = U_\mu(x)U_\nu(x + \hat{\mu})U_\mu^\dagger(x + \hat{\nu})$ surrounding it:

$$U_\mu(x) \rightarrow \mathcal{P}[\alpha U_\mu(x) + \gamma \sum_\nu U_\mu^\nu(x)]. \quad (1)$$

Here \mathcal{P} denotes the projection onto the gauge group (for $SU(2)$ just a rescaling of the matrix by a scalar). We choose $\alpha = 0.55$ and $\gamma = 0.075$, following [2]. Cooling is obtained by ignoring the old link ($\alpha = 0$) and is known to drive the configurations towards classical solutions.

A more recent idea for **filtering** is to use eigenmodes of lattice Dirac operators. Generally speaking, their function as filters is based on the argument that low-lying eigenmodes tend to be smooth, see Fig. 1 for an example. The positions revealed by the lowest-lying modes are expected to be correlated with the location of the relevant gluonic IR excitations, in particular of topological objects [3]. Whether peaks show up at the same locations when gluonic filtering methods are applied, is an important consistency check for the latter.

The **Dirac filtering** method relies on the representation of gluonic observables through eigenmode expansions of lattice Dirac operators (see also [4]). In the following we will investigate the topological charge density [5] in terms of eigenmodes of a Ginsparg-Wilson type

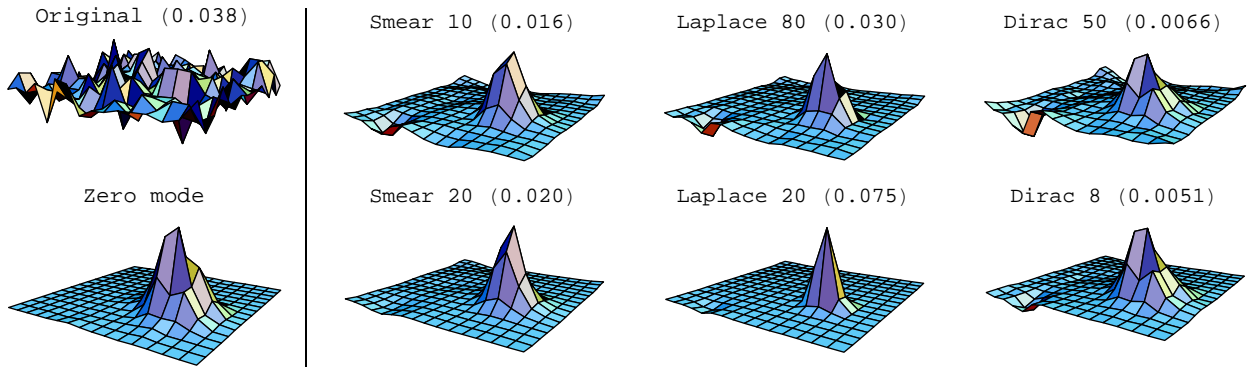


FIG. 1: Effect of different filtering methods on the topological density for a particular $Q = 1$ configuration in a fixed lattice plane. On the far left we show the original topological density (top) and the profile of the chiral zero mode (bottom), to be compared with the improved gluonic topological density after smearing (second column) and Laplace filtering (third column) and the topological density in terms of Dirac eigenmodes (last column). Results corresponding to mild and strong filtering are shown in the top and bottom row, respectively. The numbers in brackets give the heights of the corresponding maxima.

Dirac operator D :

$$q(x) = \text{tr} \gamma_5 \left(\frac{1}{2} D_{x,x} - 1 \right) = \sum_{n=1}^N \left(\frac{\lambda_n}{2} - 1 \right) \psi_n^\dagger(x) \gamma_5 \psi_n(x) \quad (2)$$

which is exact for $N = 4N_c \cdot \text{Vol}$ and can be truncated for filtering purposes at low N [6]. The total topological charge $Q = \sum_x q(x)$ is an integer given by the contributions of chiral zero modes, whereas the non-zero modes modify the local distribution $q(x)$ only.

The third filtering method we use is the **Laplace filter** that represents link variables through a spectral sum [7]

$$U_\mu(x) = \mathcal{P} \sum_{n=1}^N (16 - 2\lambda_n) \phi_n(x) \otimes \phi_n^\dagger(x + \hat{\mu}). \quad (3)$$

Here, ϕ_n are the eigenmodes of the gauge covariant Laplace operator $-D^2[U]$ with eigenvalues λ_n , of which again only the lowest N are taken into account. In the limit $N = N_c \cdot \text{Vol}$ the original links would be reproduced. Numerically this filter is cheaper than Dirac operators.

The strength of the filters can be controlled. More iterations of smearing or less eigenmodes result in a stronger filtering. We also remark that smearing is a strictly local procedure, while working with eigenmodes introduces an intrinsic nonlocality.

Results

We have generated 295 independent quenched $SU(2)$ configurations on a 16^4 lattice with tree-level Lüscher-Weisz action at $\beta = 1.95$ (the lattice spacing is 0.13 fm). We use chirally improved fermions [8], an approximate solution of the Ginsparg-Wilson relation, which reveal chiral properties well enough without the big computational demands of, e.g., overlap fermions.

The main physical observable for our comparative study is the topological charge density. For smearing and

the Laplace method, which both provide filtered links, we use the gluonic definition $q(x) = \sum_{\mu,\nu} \text{tr} F_{\mu\nu} \tilde{F}_{\mu\nu} / 16\pi^2$ with an improved field strength $F_{\mu\nu}$ constructed from 1×1 , 2×2 and 3×3 Wilson loops [9]. The Dirac eigenmodes yield $q(x)$ directly via Eq. (2).

In Fig. 1 we show the result of the three methods realizing two levels of filtering (mild and strong, see later) on a thermalized $Q = 1$ configuration in a fixed lattice plane. It shows an excellent agreement of the ‘hot spots’, i.e., lattice locations with large local topological charge, visible through the various methods. For mild filtering also less pronounced structures appear, which agree between the methods (and are washed out by strong filtering).

Moreover, the most pronounced structure corresponds to a maximum in the profile of the chiral zero mode. From this consistency we can conclude that differences between the methods are small.

The configuration used in Fig. 1 has unit topological charge, following from the existence of a single chiral zero mode. The following table shows how smearing and Laplace filtering recover this fact:

smearing		Laplace filtering	
sweeps	Q	Q	modes
1	0.948*	1.161*	160
2	1.256*	0.947*	80
5	1.118*	0.896*	40
10	1.004*	0.778*	20
20	1.000*	0.760*	10
80	1.000*	-0.138	4

The main conclusion here is that the three methods agree on the total charge $Q = 1$. Furthermore, Q evaluated after smearing approaches 1 rather quickly and then is stable. It also keeps the chiral zero mode (marked with asterisks * in the table). The Laplace-filtered configurations, on the other hand, are not arbitrarily smooth, such

that the gluonic topological charge measured on them is 1 within some margin; on the configurations filtered with 10 or more modes we find again one chiral zero mode confirming $Q = 1$.

The example discussed so far is typical for the whole ensemble (incl. all Q -values) and visualizes the impressive similarity of smearing, Laplace filtering and Dirac eigenmodes, which in the following will be quantified.

In particular we try to set the parameters of the filtering methods such that the results match as good as possible. For that purpose we consider correlators of the topological charge density (with its average $\bar{q} = Q/\text{Vol}$ subtracted):

$$\chi_{AB}(r) = \frac{\sum_{x,y} (q_A(x) - \bar{q}_A)(q_B(x) - \bar{q}_B)\delta(|x - y| - r)}{\sum_{x,y} \delta(|x - y| - r)} \quad (4)$$

depending on the four-dimensional distance r . A and B stand for the filtering methods under consideration (including their parameters).

As Fig. 2 shows, the auto-correlators $\chi_{AA}(r)$ have a positive profile over a few lattice spacings followed by a slightly negative tail, and the cross-correlators $\chi_{AB}(r)$ fall in between them. The ratio of the latter to the geometric mean, $\Xi_{AB} = \chi_{AB}^2(0)/(\chi_{AA}(0)\chi_{BB}(0))$, being close to 1 signals local agreement between the topological charge landscapes of methods A and B .

Fig. 3 shows Ξ_{AB} for pairwise comparisons of smearing, Laplacian and Dirac filtering¹. In all pairs of methods Ξ_{AB} reveals a ‘ridge’ on which the parameters match best. From mild filtering (lower left corner²) to stronger

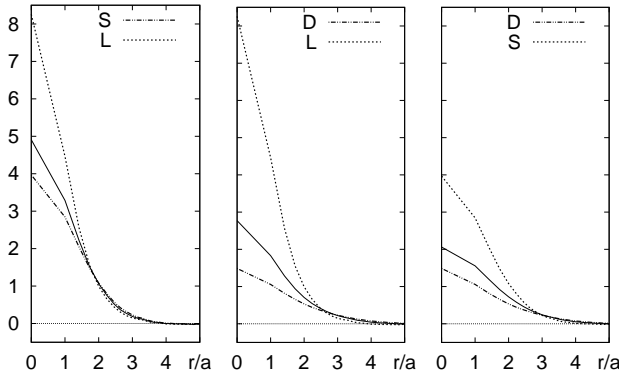


FIG. 2: Auto-correlators $\chi_{AA}(r)$ (broken lines) and cross-correlators $\chi_{AB}(r)$ (full line) of smearing (S), Laplace (L) and Dirac (D) filtering for the configuration of Fig. 1 at mild filtering. The unit on the vertical axis is 10^{-7} .

¹ Investigations that need 50 Dirac modes are done on an ensemble of 10 configurations for computational reasons.

² From the definition it follows that in the limit of no smearing sweeps vs. $N_C \cdot \text{Vol}$ Laplacian modes one has $\Xi_{AB} = 1$.

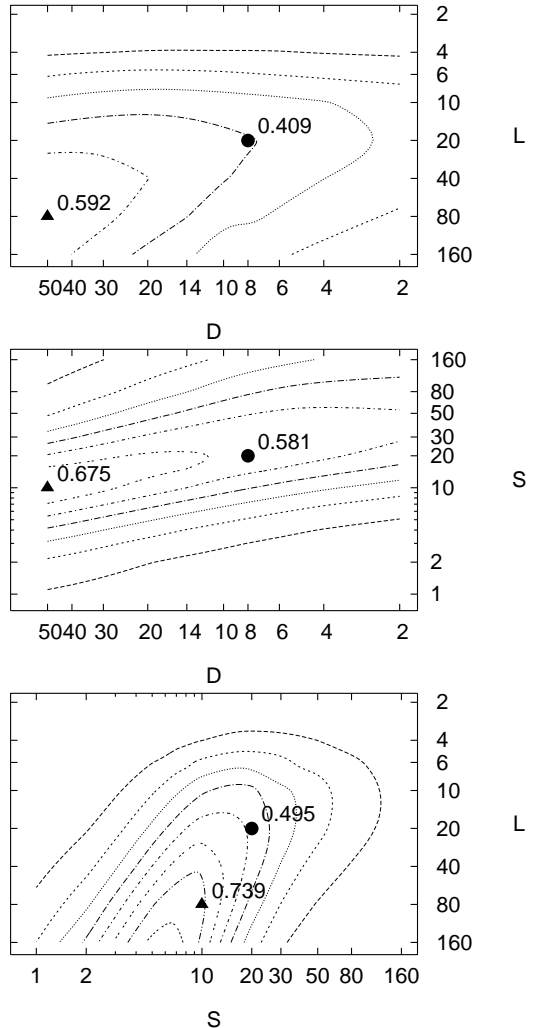


FIG. 3: Level curves $\Xi_{AB} = 0.1, 0.2, \dots$ (inwards) for A and B being smearing sweeps (S), Laplacian (L) and Dirac (D) eigenmodes, averaged over 10 configurations. The parameter sets we use at mild and strong filtering are indicated by a full triangle and a circle, respectively.

filtering (upper right corner) the methods deviate from each other and the height of the ridge decreases. Two optimal parameter sets chosen from that figure (and indicated in it) are used in due course:

	smearing	Laplace	Dirac
mild filtering	10 sweeps	80 modes	50 modes
strong filtering	20 sweeps	20 modes	8 modes

These matchings have also been confirmed by comparing smeared and Laplace-filtered links minimizing $\sum_{x,\mu} \text{tr}(U_\mu^A(x) - U_\mu^B(x))^\dagger (U_\mu^A(x) - U_\mu^B(x))$.

For these two optimal parameter sets we summarize in the following table some additional measurements, which characterize the deviation of the smeared and Laplace-filtered ensemble from the original Monte Carlo one (295

configurations). The observables are the percentage of configurations for which the topological charge Q coincides with the number of zero modes (called Q_D), the action S and the string tension σ :

	$ Q - Q_D \leq 0.5$	S/S_{orig}	$\sigma/\sigma_{\text{orig}}$
10 sweeps	89%	0.026	0.38
80 modes	76%	0.036	0.40
20 sweeps	85%	0.009	0.31
20 modes	69%	0.017	0.35

In reducing the noise, the action has been reduced by approximately two orders of magnitude, while a reasonable fraction of the string tension is kept.

With the parameter sets at hand we further quantify the local agreement of the methods by looking at clusters of filtered topological charge. For each method A cuts in the topological charge are adjusted such that the sets X_A of points above the cut have the same volume fraction $f = \text{vol}(X_A)/\text{Vol}$. Then we compare the volume in the overlap (with same sign of topological charge) vs. the union of pairs X_A and X_B to obtain the relative point overlap (RPO) s_{AB} :

$$s_{AB} = \sum_{\substack{x \in X_A \cap X_B \\ q_A(x)q_B(x) > 0}} 1 / \sum_{x \in X_A \cup X_B} 1. \quad (5)$$

In Fig. 4 (top) the RPOs are plotted against the volume fraction f . The main result to emphasize here is that the pairwise point overlaps are large, typically 50% to 60%, and constant over a wide range of f , which implies that also the shapes of the topological lumps agree.

Based on our analysis we are able to discard artefacts of the individual methods. When we analyze only points that are common to all three methods, the number of clusters is reduced accordingly, see Fig. 4 (bottom).

Intermediate values of f are suited for a cluster analysis as they contain enough statistics and avoid cluster mergings. Interestingly, in that regime we find for the common structures a pronounced power-law for the number of clusters as a function of f . A simple model of a dilute gas of topological lumps of dimensionality δ and size distribution $d(\rho) = \rho^\beta$ gives such a power-law profile-independently, with exponent $(1 + \delta/(\beta + 1))^{-1}$. Beyond the power law region the filtered topological charge tends to aggregate into two large clusters of opposite sign. A more detailed analysis of these observations will be given in a future publication.

Conclusions

We have presented a systematic comparison of filtering methods on the lattice, namely the gluonic smearing update and truncated expansions based on Laplacian and Dirac eigenmodes. Our finding, that these filtering methods agree surprisingly well, allows to identify structures of interest nearly free of artefacts.

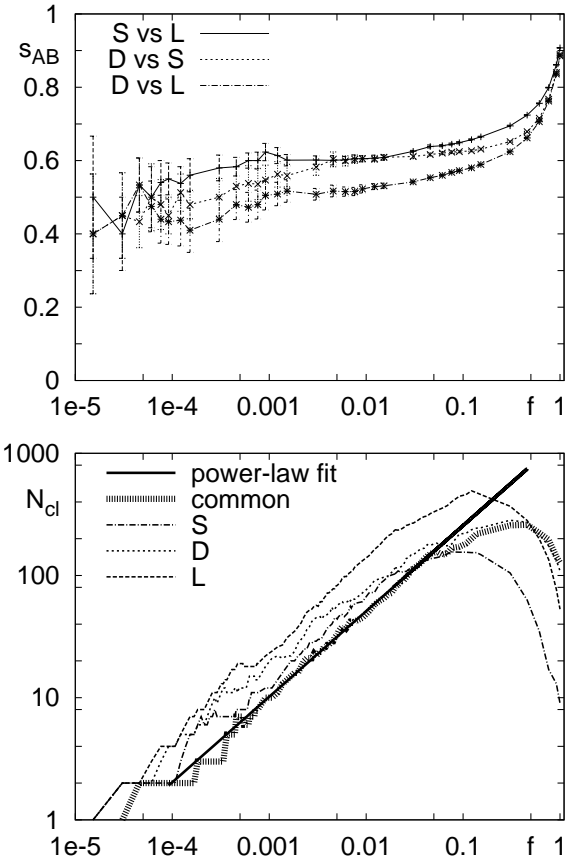


FIG. 4: RPOs averaged over 10 configurations (top) and logarithm of the number of clusters for the configuration of Fig. 1 (bottom, including a power-law fit), both as a function of the volume fraction f at mild filtering.

We have shown how to match the parameters of the methods optimally and in that spirit propose to cross-check all filtering results obtained in the future.

This work has been supported by DFG (Forschergruppe ‘Gitter-Hadronen-Phänomenologie’) and BMBF.

- [1] G. ’t Hooft, hep-th/0010225.
- [2] T. DeGrand, A. Hasenfratz, and T. G. Kovacs, Nucl. Phys. **B520**, 301 (1998).
- [3] C. Gattringer, E.-M. Ilgenfritz, and S. Solbrig, hep-lat/0601015.
- [4] C. Gattringer, Phys. Rev. Lett. **88**, 221601 (2002).
- [5] F. Niedermayer, Nucl. Phys. Proc. Suppl. **73**, 105 (1999).
- [6] I. Horvath et al., Phys. Rev. **D68**, 114505 (2003), E.-M. Ilgenfritz et al., Nucl. Phys. Proc. Suppl. **153**, 328 (2006).
- [7] F. Bruckmann and E.-M. Ilgenfritz, Phys. Rev. **D72**, 114502 (2005).
- [8] C. Gattringer, Phys. Rev. **D63**, 114501 (2001), C. Gattringer, I. Hip, and C. Lang, Nucl. Phys. **B597**, 451 (2001).
- [9] S. O. Bilson-Thompson, D. B. Leinweber, and A. G. Williams, Ann. Phys. **304**, 1 (2003). hep-lat/0203008.